




Cite this: *RSC Adv.*, 2024, 14, 27520

Preparation and characterization of a ciprofloxacin-loaded nanoparticles incorporated polymeric film dressing†

Omar A. Alsaidan,^a Naveed Ahmad,^b  ^{*}a Hasan Ejaz,^b Muhammad Ajaz Hussain,^c  ^c Aameeduzzafar Zafar^a and Hassan H. Alhassan^b

In an effort to prepare a modern polysaccharide-based dressing for sustained/prolonged delivery of the antibacterial agent to prevent and control skin wound infection, ciprofloxacin (CP)-loaded sodium alginate (SA)–chitosan (CS) nanoparticles (NPs) were incorporated into novel arabinosylan (AX)–pectin (PC) blended polymeric films by solvent casting. The CP-NPs were prepared by a two-step ionic interaction method with < 300 nm size, about 25 mV zeta potential, 74% CP-loading efficiency, and approximately round shape. The CP-NPs were incorporated in optimized AX–PC polymeric film prepared by using 2% AX and 2% PC with a plasticizer (2% glycerol) and then these films were characterized for suitability as a film dressing. The transparency, improved mechanical strength, thermal stability, water transmission, and exudate uptake characteristics indicated that CP-NPs incorporated AX–PC polymeric films were suitable for dressing applications. The CP-NPs incorporated AX–PC films exhibited sustained CP release (90% release in 36 h) and better antibacterial susceptibility as compared to free CP-containing AX–PC films. Thus, CP-NPs incorporated AX–PC films are promising dressing materials to prevent and control wound infection with prolonged antibiotic release.

Received 21st April 2024
Accepted 26th August 2024

DOI: 10.1039/d4ra02951h

rsc.li/rsc-advances

Introduction

Human skin is the soft tissue that constitutes approximately above 1/6th of the total weight of the human body and is therefore considered the largest body organ.¹ The skin mainly functions as a barrier between the external and internal environment of the body and is involved in shielding the body from chemical, mechanical, physical, and microbial effects.^{1,2} In addition, the skin plays a key role in regulating temperature, metabolism, and sensing. However, the resistant functions of the skin are disrupted in wounded skin caused by mechanical, chemical, medical, or thermal injury and surgical procedures.^{1–3} The intrinsic self-healing capability of the skin is inadequate to deal with severe chronic wounds that may lead to amputation and mortality in some patients.¹ Therefore, to augment the intrinsic healing capability of skin and protect wounds from the external environment, numerous traditional/passive and modern interactive/bioactive dressing materials have been

developed and used on the wounded skin.^{1,3,4} The intrinsic multi-step process of wound-healing of the skin, which comprises hemostasis, inflammation, proliferation of cells, and remodeling, is frequently challenged by bacterial growth that may not only delay the healing but also result in severe life-threatening consequences like septicemia.^{3,5} If the wound infections are not prevented/controlled in the initial stages, the growth and aggregation of the bacteria may result in the formation of biofilms which further complicate the healing due to increased antibiotic resistance.^{6,7}

Polymeric nanoparticles (NPs) loaded with antibacterial agents hold the potential to control and treat wound infections by directly releasing antibiotics in the infected skin area and prolonging (sustaining) the duration of action thereby reducing the dose and bacterial antibiotic resistance.^{8–10} In the past decade, numerous polymeric and inorganic NP-based materials have been explored and developed for the healing of various skin wound types, reviewed comprehensively previously.^{1,3,7–9,11} The incorporation of polymeric NPs in various types of wound dressing materials (films, hydrogels, wafers, sponges, and electrospun fibers) provides an efficient and safe way to treat infected wounds.^{1,9} In this context, carbohydrate-based polymers (polysaccharides) have been extensively investigated to fabricate polymeric NPs as well as dressing materials to incorporate and apply NPs to the infected skin wound.^{1,7} The polysaccharides are employed in the fabrication of dressing materials because they possess many intrinsic salient features that are the requirements

^aDepartment of Pharmaceutics, College of Pharmacy, Jouf University, Sakaka 72388, Aljouf, Saudi Arabia. E-mail: naveedpharmacist@yahoo.com; nakahmad@ju.edu.sa

^bDepartment of Clinical Laboratory Sciences, College of Applied Medical Sciences, Jouf University, Sakaka 72388, Saudi Arabia

^cCentre for Organic Chemistry, School of Chemistry, University of the Punjab, Lahore 54590, Pakistan

† Electronic supplementary information (ESI) available. See DOI: <https://doi.org/10.1039/d4ra02951h>



of ideal dressing materials including biocompatibility, biodegradability, exudate absorption, water permeability, non-toxicity, gaseous exchange, and above all providing optimal moist healing environment.^{3,7,12} In recent decades numerous polysaccharide-based modern interactive/bioactive dressing materials have been designed and employed as wound dressings.^{3,13,14} In this regard, polysaccharide-based films (prepared by solvent casting) exhibit numerous features required in ideal dressing.^{3,14} Additionally, NPs can be easily incorporated into the film to apply to skin wounds.^{13,15–17}

Among the polysaccharides, arabinoxylan (AX) extracted from the *Plantago ovata* (*P. O.*) seeds husk, is a promising polysaccharide (consisting of xylose backbone and arabinose side chain) that has demonstrated various characteristics required in the polymeric film dressings.^{18–20} Previously, film dressings prepared by combining AX and other polymers exhibited promising features for wound healing including the potential to uptake exudate and deliver/release antibacterial agents in a wound environment.^{21–24} However, the duration of the release of the antibacterial agents from AX-based films is required to be improved along with the mechanical properties of these films. Therefore, in this study, novel AX films are prepared by combining it with an anionic polysaccharide pectin (PC) which is obtained mainly from citrus fruits and is composed of esterified galacturonic acid.^{16,25} PC is widely explored for preparing dressing materials (in combination with other polymers) that are attributable to its biodegradable, biocompatible, and exudate swelling characteristics.^{26,27} Moreover, to sustain the antibiotic release, antibiotic-loaded sodium alginate (SA)–chitosan (CS) NPs were incorporated in AX–PC films. Both SA (anionic polysaccharide) and CS (cationic polysaccharide) have been extensively explored for the delivery of therapeutics, the preparation of NPs, and the preparation of different types of dressing materials owing to their biocompatibility, water absorptivity, biodegradability, and mucoadhesiveness.^{1,13–15,17} Previously, the SA–CS NPs could be prepared simply by electrostatic interaction without using any toxic/harsh chemicals/solvents.^{28,29} Ciprofloxacin (CP) (second-generation fluoroquinolone), is commonly employed as a model antibiotic in the development of antibacterial NPs and dressings mainly owing to the broad-spectrum antibacterial activity of CP against both Gram-positive (+ve) and –negative (–ve) organisms.^{13,14,30}

Herein, we report the preparation of CP-loaded SA–CS NPs by electrostatic interactions for their incorporation into the polysaccharide (AX–PC) films. The prepared NPs and NPs containing AX–PC films were characterized for their physiochemical properties, and suitability as wound dressing material. Moreover, the ability of the CP-NP incorporated films to sustain the release of antibiotic (ciprofloxacin) in the wound site and their antibacterial effect against wound infection-causing bacteria was also investigated.

Experimental

Materials

Ciprofloxacin (HCl), SA, PC from the citrus peel, NaOH, HCl, glycerol, CaCl₂, and PBS were supplied by Sigma-Aldrich (St.

Louis, MO, USA). Chitosan (ultra-low molecular weight) was procured from (Glentham Life Sciences, Germany) while *P. O.* seed husk (Kamal & Sons, India) was purchased from the local market.

Preparation of nanoparticles (SA–CS NPs)

Sodium alginate–chitosan (SA–CS) nanoparticles (NPs) were prepared using a previously optimized two-step electrostatic interaction method with slight modifications.²⁸ Briefly, in the first step, SA pre-gel was prepared by dropwise addition of 2 mL CaCl₂ solution (0.5 mg mL^{−1}) in 10 mL SA solution (0.6 mg mL^{−1}, pH 5.1) with constant stirring at 900 rpm at 25 °C. The formed pre-gel was continuously stirred for half an hour and large aggregates were broken by utilizing bath sonication for 30 minutes (without heating). After that, in the second step, CS solution (0.3 mg mL^{−1} in 1% acetic acid, pH 5.4) was slowly added to pre-gel in an equal SA to CS ratio (1 : 1) under constant stirring at 900 rpm. The resultant SA–CS complexes were equilibrated for 12 h to let the formation of compact and equally sized SA–CS NPs. In order to prepare CP-loaded NPs, CP solution was added to CS solution (with final CP concentration 0.05% w/v) and then this CP–CS solution was added to pre-gel to prepare CP-loaded NPs (CP–NPs),³⁰ as described above. The blank and CP-loaded SA–CP NPs dispersions were centrifuged for 30 min at 5000 rpm to separate large aggregate (as pellets) and NPs (present in supernatant). The supernatant was then centrifuged for 20 min at 5000 rpm using a filter centrifuge tube (Ultracel-100K) for removal of free CP and polymers (separation of NPs).³⁰

Characterization of SA–CS NPs

The blank and CP-loaded NPs were characterized for size, charge, morphology, and chemical structure before incorporation into AX–PC films. The size, poly-polydispersity index (PDI), and surface charge (zeta potential) of blank and CP-loaded SA–CS NPs were measured using Zetasizer equipment (Nano ZS, Malvern Instruments Ltd, Worcs, UK). Whereas, to study the morphology of the SA–CS NPs, a Field Emission Scanning Electron Microscope (FESEM) (Inspect S50, FEI, Brno, Czech Republic) was utilized. Briefly, the dispersion of SA–CS NPs was diluted 100× and then 20 µL was dropped on a silicon slip and dried under air at 25 °C. These samples were spur-coated with gold (Quorum, Q150 R ES, UK) and micrographs were captured at 20 kV. The chemical interactions among SA, CS, and CP were investigated using FTIR-ATR spectrophotometry (FTIR-7600, Lambda Scientific, Magill, Australia). The IR spectra of SA–CS NPs were obtained over a wavenumber range of 4000–500 cm^{−1}.

The loading efficiency (LE%) of CP in SA–CS NPs was determined by centrifuging the CP-loaded SA–CS NPs at 25 000 rpm for 40 min and determining the CP concentration in the supernatant by a UV-vis spectrophotometer (Genesys 10s, Thermofisher scientific, MA USA) at 276 nm. The CP LE% was calculated using the following equation:^{15,30}

$$\text{LE(\%)} = \frac{\text{Total CP} - \text{CP in supernatant}}{\text{Total CP}} \times 100$$



Preparation of arabinoxylan–pectin (AX–PC) polymeric films

Polymeric films of AX and PC were prepared by solvent casting, as reported earlier.²¹ Initially, the optimal formulation to cast AX–PC films was investigated by varying the composition of AX, PC, and glycerol (GL, as plasticizer) in film formulations (Table S1†). Then blank and loaded (with CP, blank NPs, and CP-NPs) films were prepared using optimized (selected) film formulations. Briefly, the 4% (w/v) aqueous stock dispersions of AX and PC were prepared separately. Then AX and PC dispersion were mixed in equal ratio (1 : 1) and 2% GL (v/v) was added with continuous stirring and 500 rpm for 30 min. Moreover, 0.05% CP, 100 mg blank NPs, and 100 mg CP-NPs were added to this AX–PC gel to cast CP, blank NPs, and CP-NPs loaded films respectively. The resulting casting gels were bath sonicated then 20 g gel was poured into 9.5 cm (diameter plates) and dried at 30 °C for 48 h. The optimal composition of AX–PC polymeric film formulations is provided in Table 1.

Characterization of the polymeric (AX–PC) films

The smoothness, transparency, peelability, and foldability of the dried AX–PC films were physically examined.²⁴ Then water evaporated (lost) in the drying process of the polymeric films was estimated by applying the earlier reported formula²³ and the thickness of the AX–PC polymeric films were measured using a manual micrometer at five different points.^{22,23}

The rate of water vapor transmission (WVT) across AX–PC polymeric films was estimated using a previously reported method.¹⁵ Briefly, about 2 cm diameter pieces of BF, CF, NF, and NCF were tied to the opening vials containing 2 g desiccant (silica gel). These vials were then held in desiccators at 82% RH (maintained by placing concentrated KCl) at 25 °C. The vials were weighed at 0, 1, 8, 16, 24, and 48 h and the WVT rate was calculated by applying the previously reported formula.²¹

The BF, CF, NF, and NCF (AX–PC) films were subjected to mechanical analysis by following ASTM standards (ASTM D882–18). For this purpose, AX–PC films were pulled (until broken) at a crosshead speed of 5 mm min^{−1} using UTM (LS5, Lloyd Instruments, SXW, UK), and tensile strength (TS) and percent elongation at break (EB%) were calculated using earlier reported method.²⁴

The FTIR-ATR analyses were conducted to investigate the chemical compatibility of the film constituents (*i.e.* AX, PC, NPs, and CP-NPs) using (FTIR-7600, Lambda Scientific, Magill, Australia). Briefly, small pieces of the BF, CF, NF, and CNF were placed on ATR assembly and scanned over a wavenumber range of 4000–500 cm^{−1} to record FTIR spectra.

The AX–PC films were analyzed by a Thermogravimetric Analyzer (TGA-50 Shimadzu, Kyoto, Japan) to understand the

thermal degradation of the AX–PC polymeric films. The small pieces of BF, CF, NF, and NCF films were weighed, and placed in the TGA pan. The weight loss of the films was studied from 30 to 600 °C temperature in 20 mL per min N₂ (g) flow and at 10 °C min^{−1} heating rate.

To observe surface morphology, the BF, CF, NF, and NCF film pieces were spur-coated with gold, and then micrographs were captured using FESEM at different magnifications.

The capacity of BF, CF, NF, and NCF films to absorb the exudate and expand in the wound surface was assessed in a 4% gelatin solution. Briefly, circular pieces (1.5 cm diameter) of the BF, CF, NF, and NCF films were added to the Petri plates filled with 20 g of 4% gelatin. The % expansions of the tested polymeric films were estimated over the next 24 h according to the previously reported equation.²²

Drug release from polymeric films

In vitro release studies of the CP from CP-loaded film (CF) and CP-NPs containing films (NCF) were performed using vertical Franz diffusion (DHC-6T) equipment supplied with electric heating and an autosampler system (Logan Instruments, NJ, USA).²¹ In the receptor, PBS (pH 7.4) was added as release media at 37 °C and a 0.45 µm membrane filter was mounted over the receptor compartment. Then CF and NCF films were placed over the membrane and the donor compartment was clamped with the receptor. At pre-set times 0.5 mL aliquots were taken from the receptor compartment by autosampler. The amount of the CP released was determined by using a UV-vis spectrophotometer at 276 nm and the release profile was plotted as percent cumulative *vs.* time. Thereafter, different mathematical (release kinetic) models were applied to assess the mechanism and kinetics of CP release from BF and NCF films, as reported earlier.²⁴

Antibacterial testing

The antibacterial test of BF, CF, and NCF films sample and pure CP solution (control) was conducted in Gram +ve (*S. aureus*) and Gram −ve (*E. coli*) bacteria frequently associated with wound infection using the “Disk diffusion method”.^{27,28} The standardized suspensions of bacteria (in nutrient broth), were spread in plates containing M–H agar. Then circular disk-shaped sample films (7 mm diameter) and CP solution (0.05%, 20 µL) dipped filter disks were applied on the bacteria-containing plates. These plates were incubated at 37 °C for 24 h and the diameter (size) of inhibition zones were observed and measured.

Table 1 The composition of optimized AX–PC film formulations

AX–PC films	Code	AX	PC	GL	CP	NPs	CP-NPs
Blank	BF	2%	2%	2%	—	—	—
CP-loaded	CF	2%	2%	2%	0.05%	—	—
Blank NPs incorporated	NF	2%	2%	2%	—	100 mg	—
CP-NPs incorporated	NCF	2%	2%	2%	—	—	100 mg



Statistical analysis

The quantitative experiments were repeated thrice and the standard deviation (SD) is reported with average. To calculate statistically significant differences ($p < 0.05$) Tukey's test, and t -test was performed by GraphPad Prism V 5.02® software.

Results and discussion

Preparation of SA-CS NPs

The blank and CP-loaded SA-CS nanoparticles were successfully prepared by a two-step electrostatic interaction method that involved the preparations of the SA pre-gel by ionotropic interaction using CaCl_2 and then complexation SA pre-gel with cationic CS solution to form SC-CS NPs.^{28,30}

Characterization of SA-CS NPs

The results of the characteristics of blank and CP-loaded SA-CS NPs are presented in Table 2. Firstly, the results of the particle size (DLS) characterization (Fig. S1†) show that the size of blank NPs and CP-NPs was found to be 285 ± 51 nm and 291 ± 45 nm with 0.405 ± 0.03 and 0.384 ± 0.05 PDI, respectively. The result indicates that the loading of CP into SA-CS NPs did not have any significant influence on the size. The size of these NPs (SA-CS) is in close agreement with SA-CS NPs prepared previously by Kaur *et al.*,²⁸ while the particle size of CP-loaded SA-CS NPs was smaller than previously the size reported by Ghaffari *et al.*³⁰ prepared by using a similar two-step electrostatic interaction preparation method. Moreover, the values of the PDI (less than

0.5) suggest uniformity in the distribution of the size in both blank and CP-loaded SA-CS NPs (with monodispersing).¹⁶

The results of zeta potential analysis show that the prepared blank and CP-loaded SA-CS NPs exhibited a zeta potential of 22.7 ± 3.7 and 25.0 ± 4.4 mV, respectively. The positive values of the zeta potential can be suggested due to the presence of the cationic CS in the NPs. The zeta-potential of the NPs is an important parameter to predict the stability of the colloidal systems as NPs with high zeta-potential value are considered more stable for long-term stability (due to particle-particle repulsion) as compared to NPs with lower zeta-potential that tend to aggregate. The zeta-potential of the prepared CP-loaded SA-CS NPs (close to +30 mV) is in close accord with earlier reported SA-CS NPs and it indicates a moderately stable colloidal system without self-aggregation.^{30,31}

The results of SEM analyses of SA-CS NPs (blank NPs and CP-NPs) are shown in Fig. 1(a) and (b). These SEM micrographs depict that SA-CS NPs (blank and CP-loaded) were about round shaped, and well dispersed/scattered without forming big aggregates. The size of blank SA-CS ranged between 160–210 nm while the size of the CP-loaded NPs was found between 190–260 nm. The size of the SA-CS particles determined by SEM is smaller than the NP size measured by DLS (zetasizer) which can be because of the drying method (air drying) of the NPs before SEM analysis.²⁸ These findings of the SEM studies of the SA-CS NPs are per previously reported SA-CS NPs.^{28,32} The FTIR-ATR analyses were employed to investigate chemical interaction among SA, CS, and CP in CP-loaded SA-CS NPs, and the resultant IR spectra are presented in Fig. 1(c). The IR spectra of the

Table 2 The characteristics of the blank and CP-loaded SA-CS NPs (average \pm SD, $n = 3$)

Sample	Particle size (nm)	PDI	Zeta potential (mV)	Loading efficiency (%)
Blank NPs	285 ± 51	0.405 ± 0.03	22.7 ± 3.7	—
CP-NPs	291 ± 45	0.384 ± 0.05	25.0 ± 4.4	74.6 ± 3.4

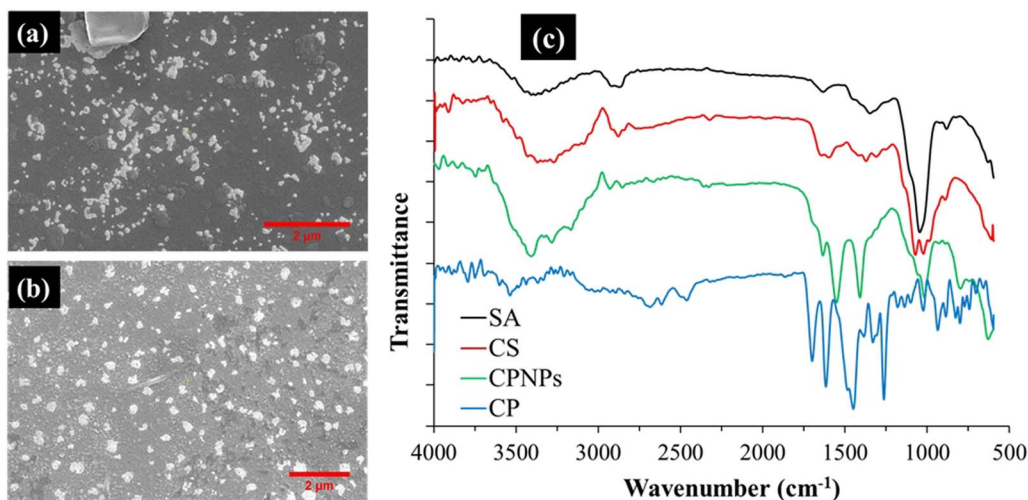


Fig. 1 SEM analyses of the, (a) blank NPs, (b) CP-NPs, and (c) FTIR spectra of SA, CS, CP, and CP-NPs.

SA, CS, and CP exhibited the characteristic peaks attributed to the functional groups present in pure polysaccharides, and fluoroquinolone (ciprofloxacin), as reported previously.^{28,32,33} The spectrum of CP-loaded SACS NPs (CPNPs) exhibited characteristic peaks of SA and CS. However, the characteristic peaks attributed to the C O stretch of the COOH and quinoline (1605), C–N stretch of the CP were shifted to lower wavenumber 1698 to 1635 cm⁻¹, 1610 to 1560 cm⁻¹ and 1467, 1452 to 1405 cm⁻¹, respectively. This shifting indicates the electrostatic complexation among the components of CP-loaded SA–CS NPs.²⁸

The loading efficiency (LE%) of CP into SA–CS NPs was calculated by determining the concentration of the CP using a UV-vis spectrophotometer. The LE of CP into SA–CS NPs was found to be 74.6% ± 3.4 (as shown in Table 1) which is higher than the previously reported CIP-loaded SA–CS NPs.³⁰

Preparation of polymeric (AX-PC) films

A suitable dressing material was required to apply CP-loaded SA–CS NPs on the infected skin wound. Therefore, novel polymeric films composed of polysaccharides AX and PC were prepared by solvent casting to incorporate the CP-loaded SA–CS NPs.²³ The results of the preliminary (optimization) studies (shown in Table S1†) suggested that the optimal films were cast by using 2% AX, 2% PC, and 1% GL (AXPC1/BF) and the BF films comply with the criteria of peelability, transparency and foldability/flexibility. Therefore, CP-loaded (CF), blank NPs containing (NF), and CP-loaded NPs containing (NCF) AX–PC films were cast by using basic BF formulation (AXPC1/BF) as given in Table 1. The optical images of these films revealed that BF, CF, NF, and NCF films are transparent, bubble-free, and slightly yellowish in color as shown in Fig. S3.†

Characterization of polymeric (AX-PC) films

The characterization of the BF, CF, NF, and NCF (AX–PC) polymeric films was performed to investigate the physicochemical properties and suitability of these films as dressing material. The results of the solvent loss, thickness, mechanical properties, and WVTR of the BF, CF, NF, and NCF films are given in Table 3.

The solvent casting method to cast polymeric film involves the pouring of the liquid blends (dispersion) of the polymers into the plastic plate and then drying this blend to constant weight. During this film casting (drying) process the solvent/liquid is evaporated leaving behind solid components in the

form of film. The amount of the solvent evaporated/lost from the casting blend provides important information about the existence of moisture in the polymeric films and the amount of solvent needed to rehydrate the polymeric films to free-flowing dispersion.^{3,22} The results of the solvent evaporation suggest that approximately 93.9% of water was evaporated from the casting blend during the drying of the BF, CF, NF, and NCF films. Moreover, the difference between the water evaporated is not significant among the different film formulations due to the same concentration of the polymer AX and PC in all film formulations. These results suggest that AX–PC films hold about 1% of the moisture and can absorb up to 90% of the liquid (wound exudate) before converting into free-flowing dispersion.²²

The determination of the thickness of the polymeric films provides significant information about the handling of the dressing as well as predicting their mechanical strength and flexibility.^{21,34} The thickness of BF, CF, NF, and NCF polymeric films ranged from 146 to 160 μm (Table 3). The statistical analyses suggested insignificant differences among the thickness of AX–PC film formulations. The nature of constituent polymers, the concentration of polymers, the volume (weight) of casting gel/dispersion, and the horizontalness of the drying surface are among the key aspects that influence the blended film thickness. The thickness of the AX–PC films is lower as compared to SA–PC^{26,34} films and AX–SA films²⁴ which can be explained due to differences in the number of polymers and volume of the liquid dispersion used to cast films. However, the results of the thickness are in close accord with our earlier reported AX-carboxymethyl cellulose films.²³

The mechanical characteristics of the dressing materials, evaluated by testing their tensile strength (T. S) and percent elongation at break (EB%), provide critical information about mechanical handling, applicability, and peeling (removal) of the dressing onto the wound area.³⁵ Among the various factors that influence the TS and %EB of the polymeric films, the thickness, interaction between the constituent polymers, and amount of the plasticizer play a key role.²⁶ The results of the mechanical characterization of the BF, CF, NF, and NCF films show that the TS of these films was between 4.5 to 4.96 N m⁻² while %EB was found between 76 to 89%. The TS of the NCF films was the highest which may be explained by electrostatic interaction among the polysaccharides present in films and NPs.²⁶ However, the difference among the TS of AX–PC films was insignificant. In contrast, the %EB of the AX–PC polymeric films

Table 3 Thickness, solvent loss, mechanical analyses, and water transmission (WVTR) of the AX–PC polymeric films (average ± SD, *n* = 3)^a

Properties	BF	CF	NF	NCF
Solvent loss (%)	93.9 ± 0.8	93.9 ± 1.1	93.8 ± 1.1	93.7 ± 0.9
Films thickness (μm)	146 ± 5.4	152 ± 6.7	158 ± 5.8	160 ± 7.8
Tensile strength (N m ⁻²)	4.51 ± 0.43	4.66 ± 0.29	4.92 ± 0.36	4.96 ± 0.43
% Elongation at break	89 ± 3.5	82 ± 5.1	76 ± 4.6*	78 ± 3.5
WVTR (g m ⁻² /24 h)	1651 ± 47	1597 ± 53	1628 ± 49	1644 ± 62

^a * denote statistically significant (*p* < 0.05) difference from BF.



was significantly decreased with the incorporation of NPs in AX-PC films (NF) indicating the increase in the stiffness of the AX-PC film in tandem with TS and thickness of films.^{23,34} The TS of CF and NCF (AX-PC) polymeric films is greater than our all earlier reported AX-based films^{21–24} and SA-PC and pluronic-PC.^{26,35} These findings of the mechanical characterization suggest that AX-PC polymeric films possess sufficient flexibility and TS required for their application as wound dressing material because TS and %EB of AX-PC polymeric films are within the limit of TS and EB of skin *i.e.* 2.5 to 16 N m⁻² and 70%.^{26,34}

The characteristic of the dressing materials to absorb and transport water without liquefying is employed to predict their capability to maintain a moist environment, transfer the exudate, and exchange dissolved gasses.^{34,35} In this regard, the estimation of WVTR of polymeric films is an important criterion to evaluate their suitability as a dressing application. The results suggest (Table 3) that the WVTR of BF, CF, NF, and NCF films was found to be 1651 ± 47, 1597 ± 53, 1628 ± 49, and 1644 ± 62 g m⁻²/24 h, respectively, without any statistically significant difference among the film formulations. This water absorption and transfer property of the AX-PC films may be suggested to the hydrophilic nature of polysaccharides AX, PC, SA, CS, and GL present in films and NPs.²¹ These WVTR values of the AX-PC films are higher than SA-PC films and in close agreement with AX-SA films are reported earlier.^{24,34} Additionally, the WVTR values of the polymeric (AX-PC) films are within the WVTR limit of the injured skin (278–5100 g m⁻²/24 h) suggesting that AX-PC films are suitable for dressing application.^{17,34}

The chemical compatibility of the AX, PC, and SA-CS NPs in the AX-PC films was confirmed using FTIR analyses. The IR spectra of BF, CF, NF, and NCF films are presented in Fig. 2(a). These spectra exhibited representative peaks of the AX, PC, CS, and SA (polysaccharides added in films and NPs) at designated wavenumber. These characteristic peaks were found in AX-PC formulation at approximately 3100–3400 cm⁻¹ (N–H, O–H stretch), 2930 cm⁻¹ (–CH stretch), 1605 cm⁻¹ (–COOH groups), 1410 cm⁻¹ (–CH₂), 1330 (O–H bending), and 1035 cm⁻¹ (C–O–C bending).^{16,23} The presence of the carbonyl stretch of amide-I of

CS at about 1700 cm⁻¹ indicates the presence of SA-CS NPs in the NF and NCF films.¹⁶ Moreover, the characteristic peaks of the CP (loaded antibiotic) were masked by polysaccharides in the CF and NCF films. These FTIR spectra of AX-PC films did not show any sign of chemical interaction among the ingredients of the films and NPs because no significant change was found in the IR peaks of polysaccharides suggesting that these polymers were chemically compatible.¹⁵

The thermal decomposition of the AX, PC, CS, CP, SA, and AX-PC films (BF, CF, NF, and NCF) was investigated using TGA to understand the influence of film formation on the thermal characteristics of the polymers. The TGA and DTG curves of the pure components are given in Fig. S4† and the films are depicted in Fig. S4(a) and (b).† AX was thermally degraded in characteristic three-steps (in agreement with our earlier findings) with maximum degradation at 335 °C.²⁴ Other pure polysaccharides *i.e.* PC, SA, and CS also underwent characteristic thermal decomposition behavior with maximum degradation at 259, 317, and 325 °C, respectively.^{24,35,36} In the TG and DTG of pure CP, the first degradation step due to the release of acetylene (C₂H₂) was recorded from 115 to 185 °C with maximum degradation at 156 °C while the second and third degradation steps were recorded from 295 to 395 °C (max at 344 °C) and 401 to 518 °C (max at 462 °C), respectively.³⁷

On the other hand, TG and DTG curves (Fig. 3(a) and (b)) of AX-PC films (BF, CF, NF, and NCF) underwent thermal degradation in one major step from about 120 to 380 °C with maxima at about 215 °C. This broad can be suggested due to the combination of the individual constituent polymers and antibiotics. Moreover, the maximum degradation of the AX-PC films was shifted towards the lower temperature as compared to pure polymers may be owing to absorbed moisture and the addition of the plasticizer (GL, which decomposes at lower temperatures). Previously, a similar decrease in the degradation of the temperature of the films was reported due to the presence of plasticizer.^{24,35}

SEM analyses of the blank (BF), CP-containing (CF), NPs-containing (NF), and CP-loaded NPs containing (NCF) AX-PC films were conducted to observe the morphology of the surface of these films. The resultant SEM micrographs captured at a magnification of 1000× are given in Fig. 4. These results suggested that the surface of BF (blank AX-PC films) was almost smooth. In contrast, the surface of CF, NF, and NCF films was rough with uniformly distributed particles that may be suggested due to the incorporation of CP and SA-CS NPs in these films.²⁴ Overall, no cracks/fissures or air bubbles were observed in all AX-PC films indicating the integrity of the films prepared.

The infected skin wound secretes exudate which should be absorbed by the dressing material. In the meantime, a dressing material should not completely dry the wound surface to augment wound healing by maintaining a moist healing environment.³⁸ Therefore, potential film dressing materials absorb exudate, expand in size, and maintain their shape without degrading.^{26,38,39} The percent expansion of the AX-PC films (BF, CF, NF, and NCF) was investigated on a gelatin surface-based simulated exuding wound model.^{23,34} The optical images of the BF, CF, NF, and NCF films captured at the start of the study

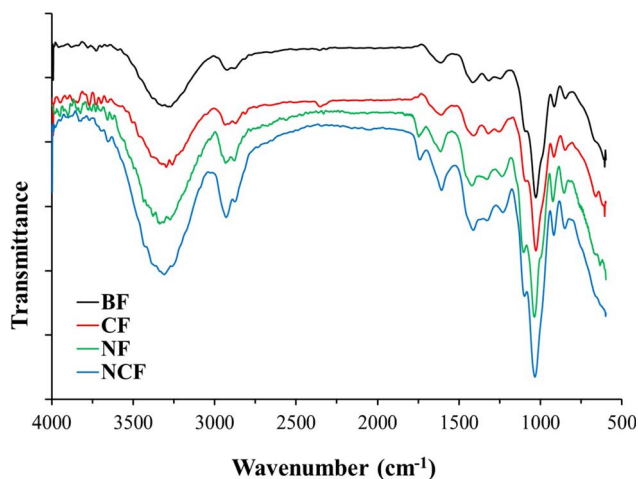


Fig. 2 FTIR spectra of the AX-PC films (BF, CF, NF, and NCF).

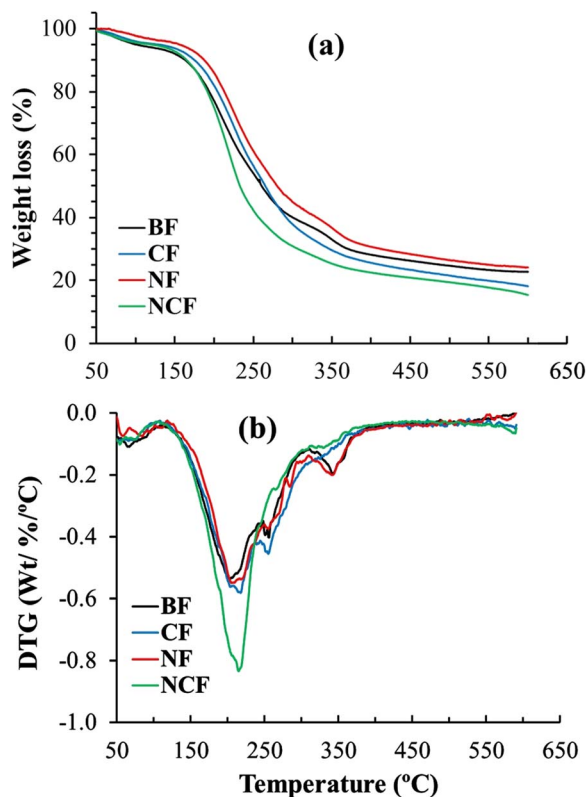


Fig. 3 (a) TG and (b) DTG curves of BF, CF, NF, and NCF (AX-PC) films.

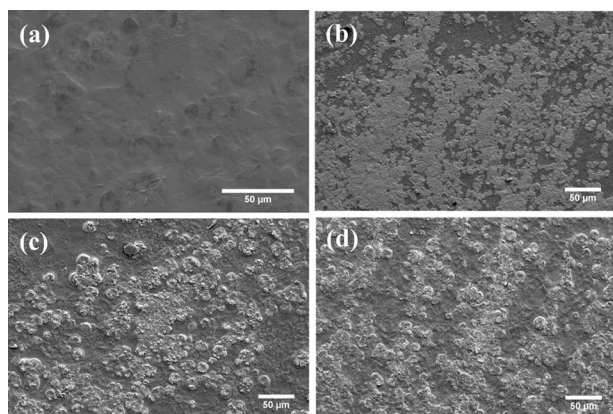


Fig. 4 SEM analyses of the surface of (a) BF, (b) CF, (c) NF, and (d) NCF of AX-PC films.

(0 h) and after 24 h are shown in Fig. 5(a) while the expansion after 24 h is presented in Fig. 5(b). These results depict the percent expansion of the BF, CF, NF, and NCF films was found to be 32.9 ± 2.9 , 31.1 ± 3.8 , 29.1 ± 3.1 and 27.4 ± 2.6 , respectively. The optical images reveal that all films were not deshaped and disintegrated after 24 h. Moreover, the percent expansion of the NPs containing films (NF and NCF) was lower than blank (BF) films which may be attributed to higher TS of NPs containing films (as discussed above). However, the difference in the percent expansion among the films was statistically insignificant. The expansion of AX-PC films was lower than our

earlier reported AXCMC²³ films and greater than AX-SA films²⁴ which may be attributed to the different nature of the constituent polysaccharides. However, the percent expansion of these (AX-PC) films is in close accord with SA-PC films, as reported earlier.^{26,34} These findings of expansion studies indicate that the AX-PC films possess the capacity to absorb wound exudate and can be appropriate for use at mild to moderately exuding wounded skin.³⁴

Drug release from polymeric films

One of the requirements of modern dressing materials is their ability to locally deliver loaded antibiotics for prolonged periods to prevent wound infection and improve patient compliance by reducing the frequency of application.³ Previously, AX and PC-based films have shown potential as dressing materials and delivery of antibiotics.^{21–24,26,35} The incorporation of antibiotic-loaded NPs in the dressing formulation prolongs the delivery duration of loaded drugs.^{2,15} Therefore, in this study, the purpose of incorporation of the CP-loaded SA-CS NPs in AX-PC films was to prolong the CP release time at the infected wound. The release of CP was investigated from CF (films containing free CP) and NCF (film containing CP-NPs) to understand the influence of incorporating CP in NPs on the release profile.

The results of release studies (shown in Fig. 5(c)) suggest CF films release approximately 90% of the total CP in 8 h whereas NCF films released about 64% of loaded CP in the same time. The total time taken by the NCF films to release 90% of the loaded CP was about 36 hours. These results indicate that CP release from the CP-NPs films (NCF) was significantly slower than films without NPs (CF). The release of the drug from the polymeric matrix requires the release media to penetrate the polymeric matrix followed by the swelling of the polymers and dissolution of the drug into the media.⁴⁰ Therefore, the release of the CP from NCF films was slower as compared to CF because first media will diffuse to films and then to NPs after that CP will first release from NPs and then it comes out of the film matrix which requires more time.²⁷ Previously, a similar increase in the drug release of drug time was observed from CS-NPs containing SA-PC cross-linked films.¹⁶ Moreover, the release of the drug form NCF was slower and prolonged as compared to our earlier reported AX-based films^{22–24} and SA-PC-based (non-crosslinked).^{26,34}

The CP release kinetics from CF and NCF films were investigated by various mathematical models. The results (Table S3†) suggest that the Korsmeyer-Peppas model was best fit with R^2 values of 0.9896 and 0.9884 for CF and NCF films, respectively. The “ n ” values of CF and NCF films were found to be 0.4603 and 0.4524 respectively suggesting that CP release was governed by the non-Fickian diffusion.⁴¹ Overall, the results of the release studies indicate NCF films with sustained CP release over a period of 36 h are suitable for dressing applications as they can prevent wound infections and improve compliance by reducing the frequency of application.

Antibacterial testing

The antibacterial activity of the AX-PC polymeric films were investigated to evaluate the potential of these films to protect/



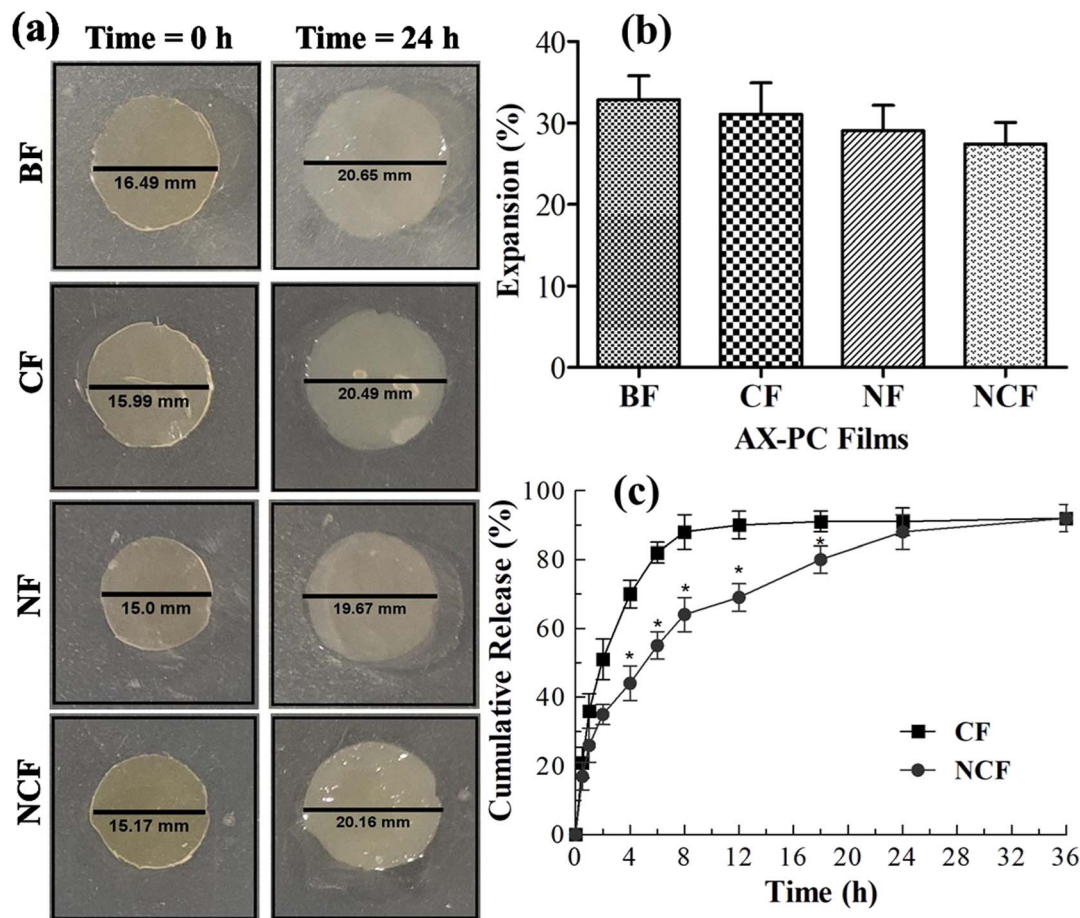


Fig. 5 (a) optical picture of films expansion, (b) percent expansion of AX-PC films (c) CP release profile of CF and NCF films.

treat wound bacterial wound infection. For this purpose, the potential of the CP-loaded (CF), and CP-NPs incorporated (NCF) films (7 mm disks) to inhibit the growth of bacteria associated with skin wound infection (*S. aureus* and *E. coli*) was evaluated on agar plates. The pure CP solution (7 mm disk) and blank (BF) AX-PC film disk were used as +ve and -ve controls, respectively (for comparison). The results indicate (Fig. 6) that the diameters of ZOI in *S. aureus* plates were measured to be 15.8 ± 2.1 , 28.9 ± 3.6 , and 26.7 ± 2.8 for CP std, NCF and CF, respectively. While CP std, NCF, and CF films exhibited ZOI 21.3 ± 2.4 , 30.3 ± 3.2 , and 27.5 ± 2.9 in *E. coli* plates. On the other hand, the blank (BF) film (negative control) did not demonstrate any ZOI against both tested strains.

These results indicate that the highest antibacterial effect was shown by films incorporated with CP-laded NPs followed by CP-loaded films and pure CP in both tested strains, respectively. Moreover, the results revealed that CP loading into NPs (NCF) and films (CF) increased its antibacterial effect as compared with control positive (CP std.). Furthermore, the antibacterial effect was found to be higher against Gram -ve (*E. coli*) than Gram +ve (*S. aureus*) strain. These results can be explained due to the presence of CP and CS in the film formulations. CP is a fluoroquinolone antibiotic that exhibits an antibacterial effect by inhibiting DNA gyrase and topoisomerase in both Gram +ve

and -ve bacterial strains.³⁰ However, sometimes its effect is lesser against *S. aureus* as in the case of this study.³⁶ The higher antibacterial activity of NCF can be explained by synergistic antibacterial effect of the CP and CS (holds intrinsic antibacterial activity). However, this synergistic effect of CP and CS on antibacterial activity was not significant which may be suggested due to the electrostatic interaction of CS with SA in NP formulation that limits the number of available NH_3^+ groups that are responsible for the antibacterial activity of CS.⁴² Overall,

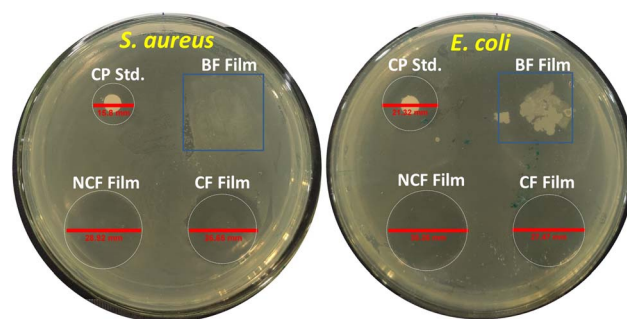


Fig. 6 Optical images of *in vitro* antibacterial test of blank (BF), CP-loaded (CF), CP-NPs incorporated (NCF) films 7 mm disks and CP std evaluated against *S. aureus* and *E. coli*.



the results of the antibacterial effect of the NCF and CF films are in close agreement with previously reported CS-loaded dressing formulations suggesting that these AX-PC films hold the potential to control skin wound infections.^{36,42}

Conclusions

In this study, CP-NPs with suitable size, charge, LE (%), and morphology were successfully prepared by the ionic interaction method. Then CP-NPs containing AX-PC films were developed with optimal formulation and evaluated for suitability as dressing material. The CP-NPs containing AX-PC films exhibited features suitable for dressing applications such as high mechanical strength, capability to uptake wound exudate, transport water vapors, and flexibility. In addition, the release of CP from CP-NPs containing films was found slower and sustained as compared release of free CP-loaded films. Finally, CP-NPs containing films exhibited better antibacterial effects as compared to pure CP solution and free CP-loaded AX-PC films. These findings allow us to conclude that the CP-NPs containing AX-PC films with optimal dressing features, prolonged CP release, and antibacterial activity are promising dressing materials for wound infections.

Data availability

The datasets supporting this article have been uploaded as part of the ESI.†

Author contributions

Conceptualization, N. A.; methodology, N. A., H. E., and O. A. A.; formal analysis, N. A. and O. A. A.; investigation, N. A., O. A. A., M. A. H., and H. E.; resources, O. A. A., H. H. A., H. E., and A. Z.; data curation, N. A. and O. A. A.; writing—original draft preparation, N. A., and O. A. A.; writing—review and editing, M. A. H., H. E., and A. Z.; supervision, O. A. A. and N. A.; project administration, O. A. A. and N. A.; funding acquisition, O. A. A. All authors have read and agreed to the published version of the manuscript.

Conflicts of interest

There are no conflicts to declare.

Acknowledgements

The authors extend their appreciation to the Deanship of Scientific Research at Jouf University for funding this work through research grant no. (DSR2020-06-3704)". The authors would like to thank the Central Laboratory at Jouf University for providing technical support for this research.

References

- 1 C. Xu, O. U. Akakuru, X. Ma, J. Zheng, J. Zheng and A. Wu, *Bioconjugate Chem.*, 2020, **31**, 1708–1723.

- 2 M. Foroutan Koudehi and R. Zibaseresht, *Mater. Technol.*, 2020, **35**, 21–30.
- 3 N. Ahmad, *Pharmaceutics*, 2022, **15**, 42.
- 4 C. D. Weller, V. Team and G. Sussman, *Front. Pharmacol.*, 2020, **11**, 155.
- 5 J. Zhou, D. Yao, Z. Qian, S. Hou, L. Li, A. T. A. Jenkins and Y. Fan, *Biomaterials*, 2018, **161**, 11–23.
- 6 J. He, Y. Qiao, H. Zhang, J. Zhao, W. Li, T. Xie, D. Zhong, Q. Wei, S. Hua and Y. Yu, *Biomaterials*, 2020, **234**, 119763.
- 7 C. Li, F. Chang, F. Gao, Y. Wang, Z. Sun, L. Zhao, Y. Yang, H. Wang, L. Dong and X. Zheng, *Appl. Surf. Sci.*, 2024, **642**, 158578.
- 8 G. Yang, M. Zhang, B. Qi, Z. Zhu, J. Yao, X. Yuan and D. Sun, *J. Biomater. Tissue Eng.*, 2018, **8**, 455–464.
- 9 M. Berthet, Y. Gauthier, C. Lacroix, B. Verrier and C. Monge, *Trends Biotechnol.*, 2017, **35**, 770–784.
- 10 N. Bag, S. Bardhan, S. Roy, J. Roy, D. Mondal, B. Guo and S. Das, *Biomater. Sci.*, 2023, **11**, 1994–2019.
- 11 N. Ahmad, S. N. A. Bukhari, M. A. Hussain, H. Ejaz, M. U. Munir and M. W. Amjad, *RSC Adv.*, 2024, **14**, 13535–13564.
- 12 P. Yudaev, Y. Mezhev and E. Chistyakov, *Gels*, 2022, **8**, 329.
- 13 D. Simões, S. P. Miguel, M. P. Ribeiro, P. Coutinho, A. G. Mendonça and I. J. Correia, *Eur. J. Pharm. Biopharm.*, 2018, **127**, 130–141.
- 14 M. Gruppuso, G. Turco, E. Marsich and D. Porrelli, *Appl. Mater. Today*, 2021, **24**, 101148.
- 15 S. Tufail, M. I. Siddique, M. Sarfraz, M. F. Sohail, M. N. Shahid, M. O. Omer, H. Katas and F. Rasool, *Curr. Drug Delivery*, 2022, **19**, 534–546.
- 16 A. Shahzad, A. Khan, Z. Afzal, M. F. Umer, J. Khan and G. M. Khan, *Int. J. Biol. Macromol.*, 2019, **124**, 255–269.
- 17 I. Savencu, S. Iurian, A. Porfire, C. Bogdan and I. Tomuță, *React. Funct. Polym.*, 2021, **168**, 105059.
- 18 S. Massey, M. S. Iqbal, B. Wolf, I. Mariam and S. Rao, *Lat. Am. J. Pharm.*, 2016, **35**, 146–155.
- 19 M. Bhatia and M. Ahuja, *Int. J. Biol. Macromol.*, 2015, **72**, 495–501.
- 20 N. Ahmad, D. Tayyeb, I. Ali, N. K. Alruwaili, W. Ahmad, A. H. Khan and M. S. Iqbal, *Polymers*, 2020, **12**, 548.
- 21 N. Ahmad, M. M. Ahmad, N. K. Alruwaili, Z. A. Alrowaili, F. A. Alomar, S. Akhtar, O. A. Alsaidan, N. A. Alhakamy, A. Zafar and M. Elmowafy, *Pharmaceutics*, 2021, **13**, 236.
- 22 N. Ahmad, D. Tayyeb, I. Ali, N. K. Alruwaili, W. Ahmad, A. ur Rehman, A. H. Khan and M. S. Iqbal, *Polymers*, 2020, **12**, 548.
- 23 N. K. Alruwaili, N. Ahmad, A. I. Alzarea, F. A. Alomar, A. Alquraini, S. Akhtar, M. S. B. Shahari, A. Zafar, M. Elmowafy and M. H. Elkomy, *Polymers*, 2022, **14**, 1769.
- 24 A. I. Alzarea, N. K. Alruwaili, M. M. Ahmad, M. U. Munir, A. M. Butt, Z. A. Alrowaili, M. S. B. Shahari, Z. S. Almalki, S. S. Alqahtani and A. V. Dolzhenko, *Int. J. Mol. Sci.*, 2022, **23**, 2899.
- 25 M. Rezvanian, N. Ahmad, M. C. I. M. Amin and S.-F. Ng, *Int. J. Biol. Macromol.*, 2017, **97**, 131–140.
- 26 M. Rezvanian, M. C. I. M. Amin and S.-F. Ng, *Carbohydr. Polym.*, 2016, **137**, 295–304.



- 27 A. P. Pandit, K. R. Koyate, A. S. Kedar and V. M. Mute, *Int. J. Biol. Macromol.*, 2019, **140**, 1106–1115.
- 28 J. Kaur, A. Kour, J. J. Panda, K. Harjai and S. Chhibber, *AAPS PharmSciTech*, 2020, **21**, 1–15.
- 29 K. L. Douglas and M. Tabrizian, *J. Biomater. Sci., Polym. Ed.*, 2005, **16**, 43–56.
- 30 S. Ghaffari, J. Varshosaz, I. Haririan, M. R. Khoshayand, S. Azarmi and T. Gazori, *J. Dispersion Sci. Technol.*, 2012, **33**, 685–689.
- 31 T. Gazori, M. R. Khoshayand, E. Azizi, P. Yazdizade, A. Nomani and I. Haririan, *Carbohydr. Polym.*, 2009, **77**, 599–606.
- 32 A. Nejabatdoust, S. D. Mirmiran, A. Salehzadeh and F. R. Masouleh, *BioNanoScience*, 2023, 1–15.
- 33 M. A. Al-Omar, in *Profiles of Drug Substances, Excipients and Related Methodology*, ed. H. G. Brittain, Academic Press, 2005, vol. 31, pp. 163–178.
- 34 C.-Y. Chin, J. Jalil, P. Y. Ng and S.-F. Ng, *J. Ethnopharmacol.*, 2018, **212**, 188–199.
- 35 T. Alavi, M. Rezvanian, N. Ahmad, N. Mohamad and S.-F. Ng, *Drug Delivery Transl. Res.*, 2019, **9**, 508–519.
- 36 M. L. Cacicedo, G. Pacheco, G. A. Islan, V. A. Alvarez, H. S. Barud and G. R. Castro, *Int. J. Biol. Macromol.*, 2020, **147**, 1136–1145.
- 37 S. H. Hussein-Al-Ali, S. M. Abudoleh, Q. I. A. Abualassal, Z. Abudayeh, Y. Aldalahmah and M. Z. Hussein, *IET Nanobiotechnol.*, 2022, **16**, 92–101.
- 38 O. Phonrachom, P. Charoensuk, K. Kiti, N. Saichana, P. Kakumyan and O. Suwantong, *Int. J. Biol. Macromol.*, 2023, **241**, 124633.
- 39 P. Jantrawut, J. Bunrueangtha, J. Suerthong and N. Kantrong, *Materials*, 2019, **12**, 1628.
- 40 A. Setapa, N. Ahmad, S. Mohd Mahali and M. C. I. Mohd Amin, *Polymers*, 2020, **12**, 2921.
- 41 P. L. Ritger and N. A. Peppas, *J. Controlled Release*, 1987, **5**, 37–42.
- 42 M. Irani, P. G. Abadi, M. M. Ahmadian-Attari, A. Rezaee, H. Kordbacheh and P. Goleij, *Int. J. Biol. Macromol.*, 2023, **128**, 634.

